Threshold values, stability analysis, and high-q asymptotics for the coloring problem on random graphs

Florent Krząkała
Dipartimento di Fisica, INFM and SMC, Università di Roma "La Sapienza," P. A. Moro 2, I-00185 Roma, Italy

Andrea Pagnani
Institute for Scientific Interchange (ISI), Viale Settimio Severo 65, I-10133 Torino, Italy

Martin Weigt
Institute for Theoretical Physics, University of Göttingen, Tammannstrasse 1, D-37077 Göttingen, Germany
Institute for Scientific Interchange (ISI), Viale Settimio Severo 65, I-10133 Torino, Italy
(Received 30 March 2004; published 29 October 2004)

We consider the problem of coloring Erdös-Rényi and regular random graphs of finite connectivity using q colors. It has been studied so far using the cavity approach within the so-called one-step replica symmetry breaking (1RSB) ansatz. We derive a general criterion for the validity of this ansatz and, applying it to the ground state, we provide evidence that the 1RSB solution gives *exact* threshold values c_q for the transition from the colorable to the uncolorable phase with q colors. We also study the asymptotic thresholds for $q \gg 1$ finding $c_q = 2q \ln q - \ln q - 1 + o(1)$ in perfect agreement with rigorous mathematical bounds, as well as the nature of excited states, and give a global phase diagram of the problem.

DOI: 10.1103/PhysRevE.70.046705 PACS number(s): 02.70.−c, 89.20.Ff, 75.10.Nr, 05.70.Fh

I. INTRODUCTION

The graph coloring problem (COL) has been studied both in combinatorics [1] and in statistical physics [2]. Given a graph, or a lattice, and given a number q of available colors, the problem consists in assigning a color to each vertex such that no edge has two equally colored end vertices. For a given graph, one quantity of interest is thereby the minimal number of colors needed, i.e., the so-called chromatic number.

In this paper we are going to consider COL as applied to random graphs of fluctuating as well as of fixed connectivity. In fact, determining their chromatic number is one of the most fundamental open problems in random-graph theory [3]. It has attracted considerable interest also within the theoretical computer-science literature: COL is one of the basic NP-hard problems which form the very core of complexity theory [1]. Defined on random graphs, the problem shows interesting phase transitions at the so-called q-COL/UNCOL thresholds c_q: Graphs of average connectivity $c < c_q$ owe proper q colorings with high probability (approaching one for graph size $N \to \infty$), whereas graphs of higher connectivity require more than q colors. This transition is connected to a pronounced peak in the numerical resolution time, i.e., in the time needed to either construct a q coloring or to prove its nonexistence. The hardest to solve problems are typically situated close to the phase boundary.

One of the first important mathematical results for q-COL on Erdös-Rényi random graphs [4] of average connectivity c was obtained by Łuczak more than one decade ago [5]. He showed in particular that, for a random graph of given finite average connectivity c, the chromatic number takes one out of only two possible consecutive values with high probability. Even if he was not yet able to determine these values, he showed that q colors are *not* sufficient for almost all graphs with $c \geqslant 2q \ln q - \ln q - 1 + o(1)$. Rephrased in terms of the q-COL/UNCOL threshold c_q, he thus proved the upper bound $c_q \leqslant 2q \ln q - \ln q - 1 + o(1)$. Very recently Achlioptas and Naor [6] put a rigorous lower bound on the threshold using the second moment method. They showed that $c_q \geqslant 2q \ln q - 2 \ln q + o(1)$, but their method in fact leads to an even better conjectured lower bound $c_q \geqslant 2q \ln q - \ln q - 2 + o(1)$ [7] which differs by just 1 from Łuczak's upper bound. So, up to these small intervals, the exact and unique value of the chromatic number is known by now. Inside these intervals, even more powerful methods are needed to determine the chromatic number and thus the COL/UNCOL threshold.

If one considers, on the other hand, the performance of linear-time algorithms, q colorings can be easily constructed up to connectivity $c \simeq q \ln q$, i.e., only in roughly the first half of the colorable phase. It is simple to design algorithms working up to $c = (1-\varepsilon) q \ln q$, for any $\varepsilon > 0$, whereas no linear-time algorithm is known which works also for connectivity $c = (1+\varepsilon) q \ln q$ [8–10]. The very existence of linear algorithms working also beyond this point is considered as another major open question [11] within the field.

Recently, the problem has been reconsidered using tools borrowed from statistical mechanics of disordered systems [12,13]. In this way both questions, i.e., the location of the q-COL/UNCOL threshold and the reason for the failure of linear-time algorithms well before this threshold, have further approached an answer, though not on completely rigorous grounds. Within the 1RSB approach, the q-COL/UNCOL transition c_q can be determined for an arbitrary number of colors q. Moreover, the 1RSB approach predicts a connectivity region $c_d < c < c_q$ inside the colorable phase, where solutions are nontrivially organized in clusters,

an exponential number of metastable states and large energetic barriers exist. This clustering phenomenon—intuitively—causes local algorithms to get stuck, see Ref. [14] for recent results.

All these results were derived with the cavity method in 1RSB approximation [15] which makes strong hypotheses on the phase space structure of the problem. The computation is further on heuristic in the sense that assumptions are only checked self-consistently, but its predictions are confirmed by independent numerical tests. Very recently a number of papers have put under scrutiny the clustering hypothesis in glass models on the Bethe lattice [16], in some combinatorial optimization problems like the random satisfiability of a formula made of the conjunction of clauses of inclusive or exclusive disjunctive combination of K boolean variable (K-SAT and K-XORSAT) as well as in polymer problems [20]. They analyze the possibility of more complex patterns of clusterization due to local instabilities.

In this work we investigate these instabilities for the coloring problem. We thereby show that a small part of the 1RSB solution of Refs. [12,13] close to the onset of the clustered phase turns out to be unstable. Interestingly enough, however, the q-COL/UNCOL transition is in the stable region at any q, and thus the 1RSB threshold results are expected to be exact. We will also analyze the stability of the coloring problem on fixed connectivity random graphs, which is somehow easier to deal with analytically.

The outline of the paper is as follows. Section II properly defines the problem under investigation, and reviews the 1RSB approach. In Sec. III we set up the general formalism for the stability analysis. The most relevant consequences of this approach for a small number of available colors are then presented in Sec. IV for the type-I instability, and in Sec. V for the one of type II. Section VI is devoted to the high q analysis of the model while, in Sec. VII, we finally consider the problem at finite energies. Conclusions and perspectives are drawn in Sec. VIII.

II. THE MODEL AND ITS 1RSB SOLUTION

A. The graph coloring problem

Let us start with a proper definition of the problem. We consider a graph $G=(\mathcal{V},\mathcal{E})$ defined by its vertices $\mathcal{V}=\{1,\ldots,N\}$ and undirected edges $(i,j)\in\mathcal{E}$ which connect pairs of vertices $i,j\in\mathcal{V}$. A graph q coloring is a mapping $\sigma:\mathcal{V}\to\{1,\ldots,q\}$ which assigns colors $1,\ldots,q$ to all vertices, such that no edges are monochromatic. For all edges $(i,j)\in\mathcal{E}$ we have therefore $\sigma_i\neq\sigma_j$.

Within the statistical-mechanics approach, a Hamiltonian is assigned to this problem such that all q colorings are found as ground states. For any color assignment, i.e., $\{\sigma_i\}\in\{1,2,\ldots,q\}$ for all $i\in\mathcal{V}$, we therefore define

$$H_G=\sum_{(i,j)\in\varepsilon}\delta(\sigma_i,\sigma_j) \tag{1}$$

with $\delta(\cdots,\cdots)$ denoting the Kronecker symbol. This Hamiltonian counts the number of monochromatically colored edges, a proper coloring of the graph thus has zero energy. In a physicist's language, the Hamiltonian describes an antiferromagnetic q-state Potts model on the graph G.

The aim within the statistical mechanics approach is to study the ground state properties of this model: If the ground-state energy equals zero, the graph is colorable. The ground-state entropy determines the number of colorings, and the order parameter, see below, characterizes the statistical properties of the ensemble of all solutions. If, on the other hand, the ground-state energy becomes positive, we know that there are no proper colorings. The graph is uncolorable with q colors.

B. Erdös-Rényi random graphs and regular random graphs

We consider the graph coloring problem on two different random-graph ensembles. The first one is the ensemble $\mathcal{G}(N,c/(N-1))$ first introduced by Erdös and Rényi in the late 1950's [4]. A graph from this ensemble consists of N vertices $j=1,\ldots,N$. Between each pair i,j of vertices, with $i<j$, an undirected edge is drawn randomly and independently with probability $c/(N-1)$. The vertices remains unconnected by a direct edge with probability $1-c/(N-1)$.

Here we are mainly interested in the thermodynamic limit $N\to\infty$, i.e., we describe large graphs of finite c. The average vertex degree, which equals the expected number of edges incident to an arbitrary vertex, is easily calculated as $(N-1)\cdot c/(N-1)=c$, and it remains finite in the large-N limit. There are, however, degree fluctuations for every finite c. In fact, in the thermodynamic limit, the probability that a randomly selected vertex has degree d, is given by the Poissonian distribution

$$p_d=e^{-c}\frac{c^d}{d!} \tag{2}$$

of mean c. Another crucial point for our analysis is that, for finite c, the number of triangles or other short loops in the graph remains finite in the large-N limit. This means that the graph is almost everywhere locally treelike, i.e., on finite length scales it looks like a tree. For $c>1$, there exists an extensive number of loops. These have, however, length $\mathcal{O}(\ln N)$, and become infinitely long for $N\to\infty$.

The second ensemble is denoted by $\mathcal{G}_c(N)$, and contains all *c-regular* graphs of N vertices, where c has to be a positive integer in this case. A graph is called c-regular if and only if *all* vertices have the same degree c, i.e., here we have

$$p_d=\delta(d,c). \tag{3}$$

A random regular graph is one randomly selected element of this ensemble. This guarantees again that the graph becomes locally treelike. Note that due to the constant vertex degree, these graphs look locally homogeneous, on finite length scales they do not show any disorder. The random character of regular graphs enters only via the long loops which are again of length $\mathcal{O}(\ln N)$. In the statistical physics literature, in particular in the theory of disordered and glassy systems, random graphs are considered as one valid definition of a Bethe lattice.

In a slightly more general context, both random graph ensembles defined before can be embedded into the en-

semble of random graphs with given degree distribution [21,22]. For these graphs, only p_d is defined, and each graph having the desired degree distribution is considered to be equiprobable. In this sense, all results formulated below can be directly generalized to arbitrary degree distributions. Sometimes the formulation will even be given in this context, but the concrete analysis will be restricted to Poissonian and regular graphs.

For this generalized ensemble, we still introduce the probability r_d that an arbitrary end-vertex of a randomly selected edge has excess degree d, i.e., it is contained in d supplementary edges, and its total vertex degree is $d+1$. Given the degree distribution, this probability results as

$$r_d = \frac{(d+1)p_{d+1}}{c}. \tag{4}$$

Plugging in our special cases, we see that this distribution remains Poissonian for Erdös-Rényi graphs, whereas the excess degrees equal constantly $c-1$ in the case of regular graphs.

C. Survey propagation equations for q coloring

The cavity equations for finite-connectivity systems in the one-step replica-symmetry broken approximation have been originally derived in Refs. [15,23]. Their single sample version is usually called survey propagation (SP) and has been introduced in Refs. [24,25] in the case of random 3-SAT. Here, in order to fix the notation, we will briefly recall the SP equations on the 1RSB level for q-COL closely following Refs. [12,13]. Note, however, that a complete explanation of all technical details is not the scope of this paper, for a detailed presentation please see therefore the original publications [12,13].

The zero-temperature properties of the system (or local minima of H_G) can be completely characterized by the edge-dependent probability distributions $[(i,j)\in\mathcal{E}]$.

$$Q_{i\to j}(\vec{u}) = \eta^0_{i\to j}\delta(\vec{u}) + \sum_{\tau=1}^{q} \eta^\tau_{i\to j}\delta(\vec{u}+\vec{e}_\tau), \tag{5}$$

where the vectors $\{\vec{e}_1,\ldots,\vec{e}_q\}$ form the usual q-dimensional canonical Euclidean base set, with components $e^\sigma_\tau=\delta(\tau,\sigma)$. The $\eta_{i\to j}$'s are positively defined probabilities, normalization implies $\Sigma^q_{\tau=0}\eta^\tau_{i\to j}=1$. The distribution $Q_{i\to j}(\vec{u})$ is called a survey, and it describes the probability that, in a suitably chosen metastable state, or local minimum of H_G, a warning $\vec{u}$ is send from vertex i via the edge (i,j) to vertex j. Possible warnings are the vectors $-\vec{e}_\tau$ which include a warning that assigning color τ to vertex i will cause an energy increase, and the zero message $\vec{u}=(0,\ldots,0)$. In the following, warnings will frequently denoted simply by their indices $\tau=0,\ldots,q$.

These distributions are self-consistently determined via the SP equations

$$P_{i\to j}(\vec{h}) = C_{i\to j}\int\left[\prod_{k\in V(i)\setminus j} d^q\vec{u}_k Q_{k\to i}(\vec{u}_k)\right] \times\delta\left(\vec{h}-\sum_{k\in V(i)\setminus j}\vec{u}_k\right)\exp\left\{y\,\omega\left(\sum_{k\in V(i)\setminus j}\vec{u}_k\right)\right\}, \tag{6}$$

$$Q_{i\to j}(\vec{u}) = \int d^q\vec{h}P_{i\to j}(\vec{h})\delta(\vec{u}-\hat{u}(\vec{h})). \tag{7}$$

There the $C_{i\to j}$ are normalization constants, the set $V(i)\subset\mathcal{E}$ contains all neighbors of vertex i, and the functions $\hat{u}$ and ω are defined as

$$\omega(\vec{h}) = -\min(-h^1,\ldots,-h^q),$$

$$\hat{u}^\tau(\vec{h}) = \omega(\vec{h}-\vec{e}_\tau)-\omega(\vec{h}). \tag{8}$$

These equations have a very nice interpretation: A site i receives an incoming field $\vec{h}$ as a sum of all but one incoming warnings. This field has either zero or negative entries, reflecting the anti-ferromagnetic character of the interaction. The maximal field components determine the colors of minimal energy if assigned to i. If this maximal field component is unique, a nontrivial message "do not take this unique color" is sent from vertex i to j via the last link. If the maximal field component is degenerate, the zero message is sent via link $i\to j$.

Note the appearance of the reweighting parameter $y>0$, which allows to scan metastable states of different energies. It acts similar to the inverse temperature in the usual Boltzmann weight: Different y concentrate the measure on different energy levels, and the limit $y\to\infty$ corresponds to zero-energy ground states.

The corresponding y-dependent free energy can be calculated as a sum of node and link contributions

$$\phi(y) = \frac{1}{N}\left[\sum_{(i,j)\in\varepsilon}\phi^{\text{link}}_{i,j}(y) - \sum_{i\in V}(d_i-1)\phi^{\text{node}}_i(y)\right], \tag{9}$$

where d_i is the degree of vertex i. The expressions for $\phi^{\text{link}}_{i,j}(y)$ and $\phi^{\text{node}}_i(y)$ are given explicitly by

$$\phi^{\text{link}}_{i,j}(y) = -\frac{1}{y}\ln\left(\int d^q\vec{h}P_{i\to j}(\vec{h})d^q\vec{u}Q_{j\to i}(\vec{u}) \times\exp\{-y[\omega(\vec{h})-\omega(\vec{h}+\vec{u})]\}\right) \tag{10}$$

and by

$$\phi^{\text{node}}_i(y) = -\frac{1}{y}\ln\left(\int\prod_{k\in V(i)} d^q\vec{u}_k Q_{k\to i}(\vec{u}_k) \times\exp\left\{y\omega\left(\sum_{k\in V(i)}\vec{u}_k\right)\right\}\right). \tag{11}$$

From this free energy we can easily calculate both the complexity $\Sigma(y)$ and the energy density $e(y)$,

$$\Sigma(y) = -y^2 \frac{\partial \phi(y)}{\partial y}, \; e(y) = \frac{\partial [y\phi(y)]}{\partial y}, \tag{12}$$

where the complexity is defined as the logarithm of the number of metastable states of energy $e(y)$, divided by the number N of vertices.

Proper colorings are characterized by the limit $y \to \infty$ of the SP Eqs. (6) and (7). In this case, positive energy contributions are forbidden and we work directly at zero energy. The SP equations can be brought into a much more handy form: They are reduced to the parameters $\eta^{\tau}_{i\to j}$, i.e., to the probabilities to have an antiferromagnetic message for color τ sent from vertex i to vertex j. Using the vectorial notation

$$\vec{\eta}_{i\to j} = (\eta^1_{i\to j}, \eta^2_{i\to j}, \ldots, \eta^q_{i\to j}), \tag{13}$$

and denoting by $V(i)\backslash j = \{k_1, k_2, \ldots, k_{d_i-1}\}$ all neighbors of i different from j, we have the closed iteration description

$$\vec{\eta}_{i\to j} = \vec{f}_{d_i-1}(\vec{\eta}_{k_1\to i}, \vec{\eta}_{k_2\to i}, \ldots, \vec{\eta}_{k_{d_i-1}\to i}) \tag{14}$$

given componentwise by

$$\eta^{\tau}_{i\to j} = \frac{\prod_{k\in V(i)\backslash j}(1-\eta^{\tau}_{k\to i}) - \sum_{\tau_1\neq\tau}\prod_{k\in V(i)\backslash j}(1-\eta^{\tau}_{k\to i}-\eta^{\tau_1}_{k\to i}) + \cdots + (-1)^{q-1}\prod_{k\in V(i)\backslash j}\eta^0_{k\to i}}{\sum_{1\leqslant\tau_1\leqslant q}\prod_{k\in V(i)\backslash j}(1-\eta^{\tau_1}_{k\to i}) - \sum_{1\leqslant\tau_1<\tau_2\leqslant q}\prod_{k\in V(i)\backslash j}(1-\eta^{\tau_1}_{k\to i}-\eta^{\tau_2}_{k\to i}) + \cdots + (-1)^{q-1}\prod_{k\in V(i)\backslash j}\eta^0_{k\to i}}, \tag{15}$$

for all $\tau \in \{1, \ldots, q\}$. The value of $\eta^0_{i\to j}$ can be calculated from the normalization constraint.

The above formalism is formulated for the analysis of a single (treelike) graph, but it can be easily modified in order to deal with average quantities on the random-graph ensembles $\mathcal{G}[N, c/(N-1)]$ or $\mathcal{G}_c(N)$, see Sec. II B. General considerations on the existence of a well defined thermodynamic limit [26,27] imply the existence of a functional probability distribution $\mathcal{Q}[Q(\vec{u})]$ describing how the surveys $Q(\vec{u})$ are distributed on the edges of the graph. Noting that a q-component vector $\vec{\eta}$ is sufficient to describe a survey $Q_{i\to j}$, we can explicitly write $\mathcal{Q}[Q(\vec{u})]$ as

$$\mathcal{Q}[Q(\vec{u})]^2 = \int d^q\vec{\eta}\rho(\vec{\eta})\delta\left[Q(\vec{u}) - \left(1-\sum_{\tau=1}^{q}\eta^{\tau}\right)\delta(\vec{u}) - \sum_{\tau=1}^{q}\eta^{\tau}\delta(\vec{u}-\vec{e}_{\tau})\right] \tag{16}$$

in terms of a simple q-dimensional probability distribution $\rho(\vec{\eta})$, with $\delta[\cdot]$ denoting a functional Dirac distribution. The SP equations (6) and (7) have to be interpreted in a probabilistic way: Drawing first an excess degree d with probability r_d, cf. Eq. (4), and then d independently chosen surveys $Q_l(\vec{u})$, $l=1,\ldots,d$, from $\mathcal{Q}[Q]$, we calculate

$$P_0(\vec{h}) = C_0 \int d^q\vec{u}_1 Q_1(\vec{u}_1)\cdots d^q\vec{u}_d Q_k(\vec{u}_d) e^{y\omega(\Sigma_{l=1}^{d}\vec{u}_d)} \times \delta\left(\vec{h} - \sum_{l=1}^{d}\vec{u}_l\right), \tag{17}$$

$$Q_0(\vec{u}) = \int d^q\vec{h} P_0(\vec{h})\delta(\vec{u} - \hat{u}(\vec{h})). \tag{18}$$

The cavity equation for the functional distribution of surveys closes by the observation that the newly generated $Q_0(\vec{u})$ has to be again a typical survey drawn from $\mathcal{Q}[Q(\vec{u})]$.

Concentrating on the color-symmetric situation $\eta := \eta^1 = \ldots = \eta^q$, the distribution $\rho(\vec{\eta})$ is reduced to a one-dimensional $\hat{\rho}(\eta)$. The limit $y \to \infty$ of the cavity equations is readily obtained:

$$\hat{\rho}(\eta) = \sum_{d=0}^{\infty} r_d \int d\eta_1\hat{\rho}(\eta_1)\cdots d\eta_d\hat{\rho}(\eta_d)\delta[\eta - \hat{f}_d(\eta_1, \ldots, \eta_d)] \tag{19}$$

with

$$\hat{f}_d(\eta_1, \ldots, \eta_d) = \frac{\sum_{l=0}^{q-1}(-1)^l\binom{q-1}{l}\prod_{i=1}^{d}[1-(l+1)\eta_i]}{\sum_{l=0}^{q-1}(-1)^l\binom{q}{l+1}\prod_{i=1}^{d}[1-(l+1)\eta_i]}. \tag{20}$$

It is also possible to give a closed expression for the complexity in the COL region (notice the p_d instead of r_d):

$$\Sigma(y=\infty) = \sum_{d=1}^{\infty} p_d \int d\eta_1\hat{\rho}(\eta_1)\cdots d\eta_d\hat{\rho}(\eta_d) \times \ln\left[\sum_{l=0}^{q-1}(-1)^l\binom{q}{l+1}\prod_{i=1}^{d}[1-(l+1)\eta_i]\right] - \frac{c}{2}\int d\eta_1\hat{\rho}(\eta_1)d\eta_2\hat{\rho}(\eta_2)\ln(1-q\eta_1\eta_2). \tag{21}$$

D. The qualitative 1RSB picture

The formalism summarized above allows to determine not only the location of the q-COL/UNCOL transition for every q, but the order parameter also allows us to extract important statistical information about structure and organization of the

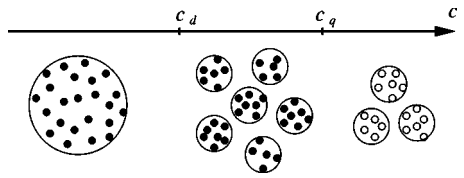

FIG. 1. A pictorial view of the solution space structure. For small average degree c, all solutions (marked by full dots) are collected within one large cluster. At some transition point c_d, this cluster breaks down into an exponential number of separated clusters. Beyond c_q, i.e., in the UNCOL phase, there are still distinct ground state clusters, but they have nonzero energy (marked by empty dots).

solutions. The most interesting point here concerns the set of solutions, seen as a subset of all q^N possible configurations $\{1,\ldots,q\}^N$. Every edge of the graph forbids a certain number of configurations. For small c, there is, however, still an exponentially large number of proper colorings. In addition, these are organized in a very simple way. They are collected in one very large cluster. For any two solutions, one can find a connecting path via other solutions, without ever changing more than $\mathcal{O}(1)$ spins within one step of this path.

This changes drastically at some average degree c_d: The set of solutions is still exponentially large, but it is split into an also exponential number of clusters. Inside each cluster, connecting paths as described above still exist, but any two clusters have an extensive Hamming distance from each other, see also Fig. 1. Technically the clustering threshold c_d is given by the first appearance of a nontrivial 1RSB solution. The number of clusters, or more precisely its logarithm divided by N, is given by the complexity (21) mentioned in the last subsection.

Inside these clusters, the first freezing phenomena are found. A large fraction of all vertices is frozen to one color in all solutions belonging to the same cluster. This color changes, of course, from cluster to cluster, since the initial model is color symmetric. Together with this clustering of ground-states, also an exponential number of metastable states appears. These have nonzero energy, but they are local minima of Hamiltonian (1).

The complexity of solution clusters decreases, until it vanishes at c_q. Beyond this point, the graph is uncolorable. There are still numerous ground state clusters, which have, however, nonzero energy but zero complexity.

III. STABILITY CONDITIONS OF THE ONE-STEP RSB SOLUTION

There is a growing believe by now that the cavity method gives exact results and not just approximations—provided that the replica symmetry is broken in the correct way. Even if a rigorous general proof is still lacking, a number of steps forward have been made so far in this direction. On this basis we conjecture that the results concerning the colorability threshold, as well as many features of the phase diagram (like for instance the existence of the clustering phase) are exact.

In general, however, the one-step RSB solution of such disordered models has no particular reason to be correct. In some models, the replica symmetry has to be broken infinitely many times to reach the exact solution. In the language of the cavity method one should thus consider an infinite hierarchy of nested clusters. This happens, for instance, in the Sherrington-Kirkpatrick (SK) model [28], and Talagrand has recently demonstrated rigorously that the RSB free energy obtained in this way is exact [29]. On the other hand there are models where 1RSB is not an approximation, and no further steps of symmetry breaking are needed. This happens, e.g., in the random-energy model [30] and in the K-XORSAT problem [31,32] (a problem known in statistical physics as the diluted p-spin model). There the 1RSB solution is known to be rigorously exact.

Here we are going to determine whether, in the q-coloring problem, one step of RSB is sufficient or whether more steps have to be taken into account to get the correct solution. We do this by means of analyzing the stability of the 1RSB solution against further RSB steps. To be more precise, we should formulate a 2RSB solution of the model and see if the 1RSB solution is stable against a small 2RSB perturbation [33]. This type of local stability analysis has receive a lot of interest recently, extending the seminal work of Elisabeth Gardner [34] to finite connectivity spin glass models [18]. It was clarified a lot in Refs. [16,20], and a formalism to deal with more general finite-connectivity problems has been established by now [16,17,19]. The coloring problem, as considered here, will allow for nice analytical treatments, in particular if considered on regular graphs.

Let us rephrase the stability considerations for our problem, following the notation in Ref. [19]. Using Eq. (16) the cavity equations for general y (17) and (18) can be rewritten in terms of the probabilities $\eta^\tau, \tau=0,\ldots,q$ only. Formally this results in

$$\eta_0^\tau = C_0 \sum_{(\sigma_1,\ldots,\sigma_d)\to\tau} \eta_1^{\sigma_1}\cdots\eta_d^{\sigma_d} e^{y\omega(\sigma_1,\ldots,\sigma_d)}, \qquad (22)$$

where the sum runs over all possible combinations of input messages $0\leqslant\sigma_1,\ldots,\sigma_d\leqslant q$ which induce the output message labeled by τ. Remember that the special case $y=\infty$ which concentrates on ground states, was given explicitly in Eq. (15).

The 1RSB solution is given by a color-symmetric distribution $\hat{\rho}(\eta)$, describing η fluctuations from link to link. Let us, for a moment, consider an arbitrary edge $i\to j$ (together with a direction) which is characterized by one *single* y-dependent value of η. In the 1RSB formalism, there are many (meta)stable states. In each of them, this link $i\to j$ carries exactly one warning corresponding either to one of the colors, or being the zero message. For a randomly selected state of energy density $e(y)$ a specific warning is found with color-independent probability η, the trivial message appears in a fraction $1-q\eta$ of these states. This is schematically represented on the left side of Fig. 2.

Let us now consider two steps of RSB. There we need to take into account the existence of clusters of states. Regarding small perturbations of the 1RSB solution, two situations are possible [18].

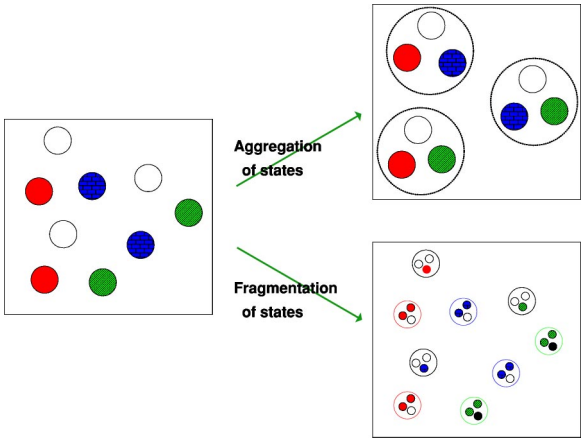

FIG. 2. (Color online) A pictorial view of the two types of instabilities of the 1RSB solution, represented here for a given link $i \to j$ in the three-coloring problem. In each 1RSB states (on the left), this link carries a message of a given color, or no message at all (white clusters here). Going from a 1RSB to 2RSB, these states may aggregate into bigger clusters (type-I instability) or fragment in new smaller clusters (type-II instability).

Type I: States may *aggregate* in configuration space, see Fig. 2. In that case the order parameter (still for a fixed link $i \to j$) is the probability $g(\eta^1, \ldots, \eta^q)$ to randomly select a cluster in which there is a fraction η^1 of states with message $-\vec{e}_1$ transmitted from i to j, etc. Note that it is not sufficient to consider a probability distribution $g(\eta)$ of a single, color-symmetric fraction η since the color symmetry can be broken inside a cluster. This is illustrated in Fig. 2. To study the stability of the 1RSB solution, one should thus write the 2RSB equation, insert a perturbed 1RSB solution and see if it evolves back to 1RSB. In this case, the 1RSB solution is obtain by considering $g(\eta^1, \ldots, \eta^q) = \delta(\eta^1 - \eta) \cdots \delta(\eta^q - \eta)$. To test stability, we thus need to replace the Dirac peaks by narrow functions of width ϵ, and to see if the width increases or goes to zero during the cavity iteration process. The analysis thus amounts to look if a small noise added to the solution will vanish. This is equivalent to testing convergence of the SP equations on a single graph. We will refer to this kind of analysis as "noise propagation".

Type II: States may fragment into new states, see the lower right picture in Fig. 2. In the 1RSB solution, a link $i \to j$ carries a message which is uniquely determined within one state. If now this state fragments into one cluster of many states, also the single message is transformed into a set of messages. To introduce a small perturbation of the 1RSB solution, we should assume that, with high probability, the states within one cluster are still characterized by the same message on link $i \to j$. In a small fraction of these states, however, also other messages may appear. The problem is now if or if not this perturbation tends to zero under iteration of the 2RSB equations. The stability analysis thus amounts to see if a change in one message (called a bug in Ref. [19]) can propagate through the whole system, or if it remains localized. We will refer to this instability, following the terminology of Ref. [19], as bug proliferation.

A. Type-I instability: Aggregation of states and noise propagation

Let us start with noise propagation. The stability can be computed from the Jacobian

$$T^{\tau\sigma} = \left. \frac{\partial \eta_0^\tau}{\partial \eta_1^\sigma} \right|_{\text{1RSB}}, \tag{23}$$

which gives the infinitesimal probability that a change in the input probability η_1^σ will change the output probability η_0^τ, cf. Eq. (22). The index 1RSB says that the expression has to be evaluated at the 1RSB solution found within the cavity approach. Note that we need to calculate this matrix only for $1 \leqslant \sigma, \tau \leqslant q$ since the probability of the zero message follows by normalization and thus does not describe an independent quantity. After one iteration, a change of one input message of a vertex of degree d induces a change in $d-1$ outgoing messages. The global perturbation after n iterations thus concerns on average $(\Sigma_d d r_d)^n$ cavity messages, where r_d is computed from Eq. (4). To monitor also the strength of the perturbation, we have to calculate

$$\sum_{d_1,\ldots,d_n} d_1 r_{d_1} \cdots d_n r_{d_n} \mathrm{tr} \langle (T_1 T_2 \cdots T_n)^2 \rangle_\eta, \tag{24}$$

where $T_1, \ldots, T_n$ are n successive T matrices. The notation $\langle \cdots \rangle_\eta$ denotes the average over the external messages to the nodes $1, \ldots, n$. To be more precise we should write $T_i = T_{d_i}(\eta_{i,1}, \ldots, \eta_{i,d_i})$, i.e., T_i depends on d_i incoming probabilities $\eta_{i,1}, \ldots, \eta_{i,d_i}$, with d_i being the excess degree of vertex i distributed according to r_{d_i}. For $i=1$, all messages are external. They have to be generated independently from the 1RSB order parameter $\hat{\rho}(\eta)$. For $i>1$, the first message described by $\eta_{i,1}$ results from node $i-1$ according to Eq. (22). The other inputs $\eta_{i,2}, \ldots, \eta_{i,d_i}$ are again external and thus independently distributed with $\hat{\rho}(\eta)$. Note that the η-averaged matrix $\langle (T_1 T_2 \cdots T_n)^2 \rangle_\eta$ still depends on the random excess degrees $d_1, \ldots, d_n$. This has to be taken into account in the sum in Eq. (24).

A simple way to calculate the trace for $n \gg 1$ is to consider the biggest eigenvalue of the matrix $\langle (T_1 T_2 \cdots T_n)^2 \rangle_\eta$, which allows us to use a single number to follow the perturbation. This, however, becomes very simple for q-COL. Let us rewrite the Jacobian

$$T = \begin{bmatrix} \frac{\partial \eta_0^1}{\partial \eta_1^1} & \frac{\partial \eta_0^2}{\partial \eta_1^1} & \cdots & \frac{\partial \eta_0^q}{\partial \eta_1^1} \\ \frac{\partial \eta_0^1}{\partial \eta_1^2} & \frac{\partial \eta_0^2}{\partial \eta_1^2} & \cdots & \frac{\partial \eta_0^q}{\partial \eta_1^2} \\ \cdots & \cdots & \cdots & \cdots \\ \frac{\partial \eta_0^1}{\partial \eta_1^q} & \frac{\partial \eta_0^2}{\partial \eta_1^q} & \cdots & \frac{\partial \eta_0^q}{\partial \eta_1^q} \end{bmatrix}_{\text{1RSB}}. \tag{25}$$

Evaluated at the color-symmetric 1RSB solution, this matrix has only two different entries: All diagonal elements are equal, and all nondiagonal elements are equal. As an immediate consequence all Jacobians commute and are thus simul-

taneously diagonalizable. The matrix T has only two distinct eigenvalues

$$\lambda_1 = \left(\frac{\partial \eta_0^1}{\partial \eta_1^1} - \frac{\partial \eta_0^1}{\partial \eta_1^2}\right)\Bigg|_{\text{1RSB}},$$

$$\lambda_2 = \left(\frac{\partial \eta_0^1}{\partial \eta_1^1} + (q-1)\frac{\partial \eta_0^1}{\partial \eta_1^2}\right)\Bigg|_{\text{1RSB}}. \tag{26}$$

The second eigenvalue belongs to the homogeneous eigenvector (1, 1,…, 1). It describes a fluctuation changing all η_1^τ, $\tau=1,\ldots,q$, by the same amount, i.e, a fluctuation maintaining the color symmetry. The first eigenvalue is $(q-1)$-fold degenerate, eigenvectors are spanned by $(1,-1,0,\ldots,0)$, $(0,1,-1,0,\ldots,0)$,…,$(0,\ldots,0,1,-1)$. The corresponding fluctuations explicitly break the color symmetry, and they are in fact found to be the critical ones for the instability of the 1RSB solution.

For zero-energy ground states in the COL phase, where $y=\infty$, one may proceed using the closed analytical expression (15) for the iteration. It is possible to explicitly write down both eigenvalues. We will see in Sec. VI how to derive asymptotic results at large q. Finally, to monitor the perturbation, one should consider the dependence of

$$\lambda_{\text{type I}}(n) = \sum_{d_1,\ldots,d_n} d_1 r_{d_1} \cdots d_n r_{d_n} \lambda_{\langle (T_1 \cdots T_n)^2 \rangle_\eta} \tag{27}$$

on the number n of iteration steps. There $\lambda_{\langle (T_1 T_2 \cdots T_n)^2 \rangle_\eta}$ denotes the biggest eigenvalue of matrix $\langle (T_1 T_2 \cdots T_n)^2 \rangle_\eta$. It can be computed as a product of eigenvalues being either all of type λ_1 or all of type λ_2. The 1RSB solution is stable against type-I perturbations if and only if $\lambda_{\text{type I}}(n)$ decays to zero in the large-n limit.

B. Type II instability: Fragmentation of states and bug proliferation

As discussed above, we have to consider bug proliferation in order to study the second type of instability, i.e., the instability with respect to fragmentation of states into clusters of states. Suppose that a message of type σ is turned into another message $\tilde{\sigma}$. This is called a bug in Ref. [19]. We suppose it to happen with small probability $\pi^{\sigma\to\tilde{\sigma}} \ll 1$. As a consequence, some output messages may change, and the bug propagates. The system is unstable with respect to type II perturbations if such a bug propagates through the whole system.

Considering small perturbations, we can work in the linear response regime. For a generic change of the first input message in Eq. (22), we may calculate the probability of changing the output message

$$\pi_0^{\tau\to\tilde{\tau}} = C_0 \sum_{\substack{(\sigma,\sigma_2,\ldots,\sigma_d)\to\tau \\ (\tilde{\sigma},\sigma_2,\ldots,\sigma_d)\to\tilde{\tau}}} \pi_1^{\sigma\to\tilde{\sigma}} \eta_2^{\sigma_2} \cdots \eta_d^{\sigma_d} e^{y\omega(\tilde{\sigma},\sigma_2,\ldots,\sigma_d)}. \tag{28}$$

This defines a matrix V with entries

$$V_{\tau\to\tilde{\tau},\sigma\to\tilde{\sigma}} = \frac{\partial \pi_0^{\tau\to\tilde{\tau}}}{\partial \pi_1^{\sigma\to\tilde{\sigma}}}, \tag{29}$$

evaluated at the 1RSB solution. Since a message may have $q+1$ different states and we are considering actual changes in messages, V is a square matrix of dimension $q(q+1)$. We study it in Appendix A and show that its biggest eigenvalues can be written, at any given y, as a function of q and $\eta_1,\ldots,\eta_d$ as

$$\lambda = (q-1)\mathcal{A}(q,\{\eta\}) + \sqrt{\mathcal{B}(q,\{\eta\})\mathcal{B}'(q,\{\eta\})}, \tag{30}$$

where $\mathcal{A}$, $\mathcal{B}$, and $\mathcal{B}'$ are explicitly given in Eq. (A4) in Appendix A. In the zero-energy case, i.e., for $y\to\infty$, this expression simplifies to

$$\lambda = (q-1)\mathcal{A}_{y=\infty}(q,\{\eta\}), \tag{31}$$

where $\mathcal{A}_{y=\infty}(q,\{\eta\})$ is given by

$$\mathcal{A}_{y=\infty}(q,\{\eta\}) = \frac{\sum_{l=0}^{q-2}(-1)^l \binom{q-2}{l} \prod_{i=2}^{d}[1-(l+2)\eta_i]}{\sum_{l=0}^{q-1}(-1)^l \binom{q}{l+1} \prod_{i=1}^{d}[1-(l+1)\eta_i]}. \tag{32}$$

The instability with respect to bug proliferation has to be determined from a product of n such matrices. Proliferation is monitored, using again Eq. (4), by

$$\sum_{d_1,\ldots,d_n} d_1 r_{d_1} \cdots d_n r_{d_n} \mathrm{tr}\langle V_1 V_2 \cdots V_n \rangle_\eta \tag{33}$$

or, using the eigenvalue notation, by

$$\lambda_{\text{type II}}(n) = \sum_{d_1,\ldots,d_n} d_1 r_{d_1} \cdots d_n r_{d_n} \lambda_{\langle V_1 V_2 \cdots V_n \rangle_\eta}, \tag{34}$$

where $\lambda_{\langle V_1 V_2 \ldots V_n \rangle_\eta}$ is the biggest eigenvalue of matrix $\langle V_1 V_2 \cdots V_n \rangle_\eta$. The averages are performed in complete analogy to averages in the type I case. The 1RSB solution is stable if and only if this eigenvalue decays to zero for $n \to \infty$.

IV. STUDY OF THE TYPE-I INSTABILITY: NOISE PROPAGATION

Using the criteria derived in the previous section, we can now study the stability of the 1RSB solution for the ground states of the coloring problem, i.e., we concentrate first on $y\to\infty$. We will, in the following, call c_{SP} the connectivity beyond which 1RSB is type I unstable because, as we will see, the SP equations do not converge anymore on a single graph for $c > c_{\text{SP}}$.

A. Regular random graphs

In the case of fixed-connectivity graphs all sites are equivalent, so η does not fluctuate from edge to edge. Therefore, the recursion equation (20) can be simplified to

TABLE I. Computation of η, Σ, and $\lambda_{\text{type I}}$ for $q=3$, 4, and 5 and various values of the connectivity on regular random graphs.

q, c	phase	η	Σ	$\lambda_{\text{type-I}}$
$q=3$, $c=4$	COL			
$q=3$, $c=5$	COL 1RSB	0.279	0.037	0.688
$q=3$, $c=6$	UNCOL Instable	0.318	−0.137	1.103
$q=3$, $c=7$	UNCOL Instable	0.327	−0.329	1.420
$q=4$, $c=8$	COL			
$q=4$, $c=9$	COL 1RSB	0.223	0.040	0.764
$q=4$, $c=10$	UNCOL 1RSB	0.236	0.03	0.86
$q=4$, $c=11$	UNCOL Instable	0.242	−0.216	1.02
$q=5$, $c=12$	COL			
$q=5$, $c=13$	COL 1RSB	0.1759	0.0960	0.5605
$q=5$, $c=14$	COL 1RSB	0.1853	0.00380	0.6788
$q=5$, $c=15$	UNCOL 1RSB	0.1902	−0.0952	0.775
$q=5$, $c=16$	UNCOL 1RSB	0.1932	−0.1982	0.8622
$q=5$, $c=17$	UNCOL 1RSB	0.1952	−0.3037	0.942
$q=5$, $c=18$	UNCOL Instable	0.1966	−0.4109	1.017

$$\eta = \hat{f}_k(\eta) = \frac{\sum_{l=0}^{q-1} (-1)^l \binom{q-1}{l} [1-(l+1)\eta]^k}{\sum_{l=0}^{q-1} (-1)^l \binom{q}{l+1} [1-(l+1)\eta]^k} \tag{35}$$

with $k=c-1$. This equation can be easily solved using basic numerical tools. Similar simplifications arise in the computation of the complexity Σ. Within the 1RSB formalism, it is therefore very easy to derive $\eta(q,c)$, to compute the corresponding complexity, and thus to determine if the graph is in the COL phase or not. One finds that that at small connectivities the solution is trivial, i.e., $\eta=0$. For $c \geqslant c_d$ the clustering RSB phenomenon occurs, and for $c \geqslant c_q$ the graph becomes uncolorable. To test the validity of the 1RSB ansatz we are now going to apply the criteria derived previously. Due to the fixed vertex degree, there is no need to average over the site distribution. The stability criterion thus simplifies considerably to

$$\lambda_{\text{type I}}(1) = k \left(\frac{\partial \eta_0^1}{\partial \eta_1^1} - \frac{\partial \eta_0^1}{\partial \eta_1^2} \right)^2 \Bigg|_{\text{1RSB}} < 1. \tag{36}$$

In Table I, we summarize the values of η and Σ, as well as stability criteria, for $q=3$, 4, and 5. The instability of type I appears at high connectivity, in the UNCOL phase. So it turns out to be irrelevant in the COL phase. This turns out to be true for arbitrary number q of colors, see Sec. VI for the asymptotic case. However, this instability is directly relevant for the behavior of the SP algorithm on single graphs: When $c \geqslant c_{\text{SP}}$, SP stops to converge on a single graph. This is actually what the Jacobian (23) implies first of all. We have verified this numerically for 3-COL, SP does not converge on regular graphs of degree equal to or larger than 6.

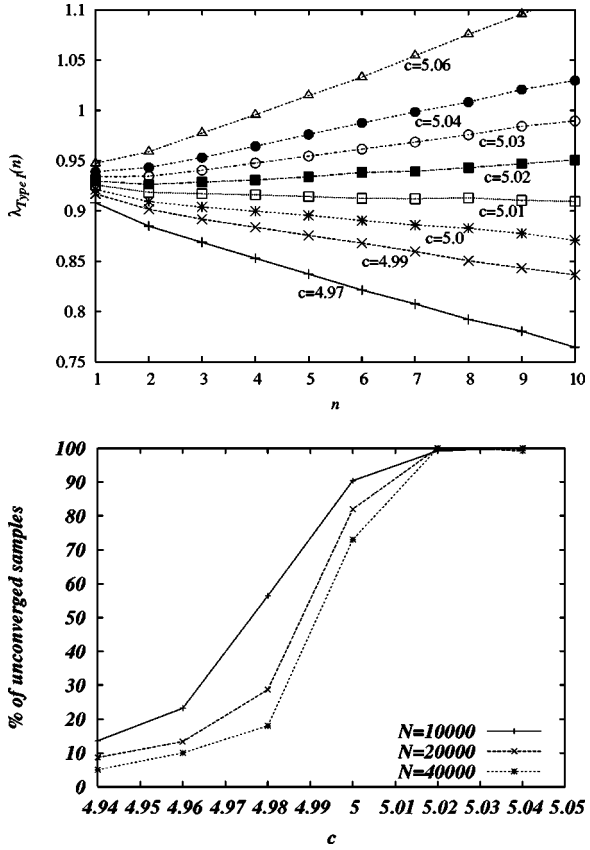

FIG. 3. (Color online) Analytic and numerical computation of the location of the type I instability point in the three coloring on fluctuating connectivities graphs. We find $c(3)_{\text{SP}} \simeq 5.01$ in both cases, which confirms well that SP equation stop to converge when $c > c_{\text{SP}}$.

B. Fluctuating-connectivity random graphs: Erdös-Rényi ensemble

Let us now turn to Erdös-Rényi random graphs. Sites are no more equivalent and the order parameters η fluctuate from link to link. We have to be very careful in the disorder average in the stability criterion, a detailed description was given above. The type I instability amounts to see if a small change in η propagates through the whole system. We saw in Sec. III that this can be computed by the study of a Jacobian that describes the propagation of a perturbation after one iteration. The global perturbation after n iteration is monitored by the sum of the squares of the perturbed cavity bias, which behaves as

$$\lambda_{\text{type I}}(n) = \sum_{d_1,\ldots,d_n} d_1 r_{d_1} \cdots d_n r_{d_n} \lambda_{\langle (T_1 T_2 \cdots T_n)^2 \rangle_\eta}, \tag{37}$$

where $\lambda_{\langle (T_1 \cdots T_n)^2 \rangle_\eta}$ is the maximal eigenvalue of the η average of matrix $(T_1 \cdots T_n)^2$. The system is stable if $\lambda_{\text{type I}}(n)$ goes to zero with n, and instable if it diverges. Let us concentrate for a moment on 3-COL: Using the SP equation on single graphs, we saw that the iteration is not converging anymore for $c > 5.01$. Evaluating the stability criterion, we were able to reproduce this number analytically (see Fig. 3). Both methods agrees exactly. We have summarized our result

TABLE II. Critical connectivities of the coloring problem on fixed connectivities random graphs.

q	c_d	c_m	c_q	c_{SP}
3	5	5	6	6
4	9	9	10	11
5	13	13	15	18
6	17	18	20	27
7	21	22	25	38
8	26	27	31	51
9	31	32	37	66
10	36	37	44	83
11	41	43	50	102
12	46	48	57	123

for c_{SP} in the last column of Table III. Again, the conclusion is that the type I instability is irrelevant for the thermodynamics of the system.

V. STUDY OF THE TYPE-II INSTABILITY: BUG PROLIFERATION

We turn now to the instability of type II. As before, we start with regular random graphs, and then we move to Erdös-Rényi graphs. In Ref. [18], it is argued that, if 1RSB states are instable, then these states should be described using a full RSB ansatz, and therefore are marginally stable [35]. The connectivity at which the instability appears was therefore called c_m for c_{marginal}. Although it is not yet clear if full RSB is needed in the case 1RSB is unstable, we follow this notation and call c_m the connectivity at which the type II instability shows up.

A. Regular random graphs

Using again the homogeneous solution, it is very easy to write the stability criterion. It reads (see Appendix B)

$$\lambda_{\text{type II}} = k(q-1)\frac{\sum_{l=0}^{q-2}(-1)^l\binom{q-2}{l}[1-(l+2)\eta]^{k-1}}{\sum_{l=0}^{q-1}(-1)^l\binom{q}{l+1}[1-(l+1)\eta]^{k}} < 1 \tag{38}$$

with $k=c-1$. Applying this criterion, it turns out that the instability does not appear at low q. In fact, for $q<6$, the ground state in the COL region is always either RS or 1RSB, no instability toward 2RSB is observed. However, when $q=6$, the lowest connectivity for which RSB appears turns out to be instable. More generally, there is an unstable zone growing with q before the stable 1RSB region is reached. We summarize our result for small q in Table II. Note that c_d is calculated in 1RSB approximation, if the latter is instable its position may change due to more-step RSB.

The one-step solution is thus *not* always stable in COL phase. It seems, however, to be correct close to the COL/UNCOL threshold, the result for the latter is therefore conjectured to be exact. The global situation is schematically represented in the Fig. 4. We have derived the solution of this problem up to $q=200$, which allows us to draw a quite complete phase diagram for the problem on finite connectivity random graphs, see Fig. 5. From this phase diagram, two important points have to be noticed.

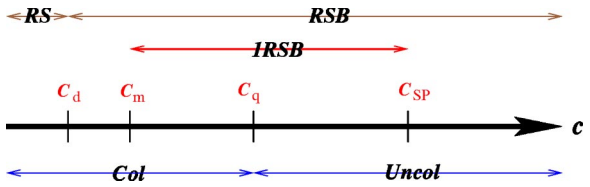

FIG. 4. (Color online) Schematic phase diagram for the coloring transition at $e=0$. At small connectivity, when $c<c_d$ the problem is COL and the space phase is trivial. Then, for $c\geqslant c_d$ the phase space is broken into many states and RSB appears. In this RSB phase there is a one-step RSB zone $c_m\leqslant c<c_{\mathrm{SP}}$ in which detailed computations are possible. The COL/UNCOL transition appearing at c_q is always found in this zone. Note that for some connectivities, c_d and c_m are equal.

The critical line for the COL/UNCOL transition is always in the 1RSB stable zone, and therefore we believe it to be be an exact result.

There are two zones where the 1RSB solution is unstable. This is happening at high connectivity in the UNCOL phase, due to a type-I instability, and also in a small, though growing (with the number of colors) zone between the RS COL and the 1RSB COL phases, due to a type-II instability.

B. Erdös-Rényi random graphs

Let us now go back to the Erdös-Rényi ensemble. As mentioned above, the instability is monitored by

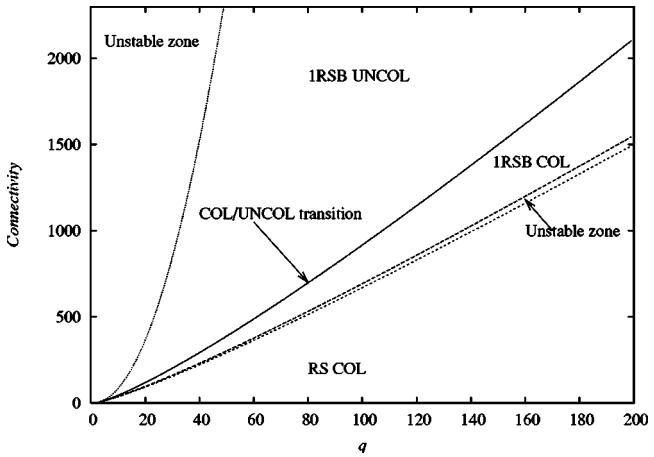

FIG. 5. (Color online) Phase diagram of the q-coloring problem on random graphs with fixed connectivities, for 3 to 200 colors. From bottom to top we have four lines corresponding to c_d, c_m, c_q and c_{SP}. The critical line c_q that separates the COL and the UNCOL region is always in the stable zone, where we conjecture our results to be exact. Note however the small, but slowly growing, zone in the COL region where the 1RSB computation is unstable.

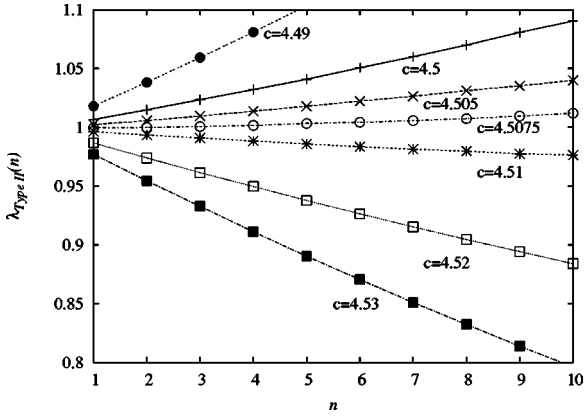

FIG. 6. Computation of the location of the type-II instability point in 3-COL on Erdös-Rënyi graphs. One finds $c_m \simeq 4.51$.

$$\lambda_{\text{type II}}(n) = (q-1)^n \sum_{d_1,\ldots,d_n} d_1 r_{d_1} \cdots d_n r_{d_n} \times \left\langle \prod_{i=1}^{n} \frac{\sum_{l=0}^{q-2} (-1)^l \binom{q-2}{l} \prod_{j=2}^{d_i} [1-(l+2)\eta_{i,j}]}{\sum_{l=0}^{q-1} (-1)^l \binom{q}{l+1} \prod_{j=1}^{d_i} [1-(l+1)\eta_{i,j}]} \right\rangle < 1, \tag{39}$$

where the d_i has the characteristic Poissonian distribution r_{d_i} of average c. As already explained above, the η values are given in the following way. For the first node $i=1$, all values of $\eta_{1,1},\ldots,\eta_{1,d_1}$ are drawn independently from $\hat{\rho}(\eta)$. This allows us to calculate the first factor in the above product, but also the first input message $\eta_{2,1}=\hat{f}_{d_1}(\eta_{1,1},\ldots,\eta_{1,d_1})$ to the second node. The other d_2-1 input messages $\eta_{2,2},\ldots,\eta_{2,d_2}$ are drawn again from $\hat{\rho}(\eta)$. This is repeated for the other vertices: The input message on the link coming from the previous node is induced via the SP equation, the others are drawn randomly. Using again the population dynamic solution of the coloring problem, it is easy to perform this average. For 3-COL, e.g., we find the instability to be present for connectivities $c<c_m\simeq 4.51$ (see Fig. 6). We have repeated this study for $q=4$ and 5. Our results are summarized in Table III. As opposed to what happens in the fixed-connectivity case, there is an unstable interval close to the clustering transition at $q=3,4$. For $q=5$, however, it is always stable. As we will see in the next section, at larger connectivities the unstable zone reappears. Again, the most important conclusion is that the critical values for the COL/UNCOL transition are in the stable zone. We thus conjecture that the connectivities for the COL/UNCOL transition are *exact*.

TABLE III. Critical connectivities of the coloring problem on Erdös-Rényi graphs.

q	c_d	c_m	c_q	c_{SP}
3	4.42	4.51	4.69	5.01
4	8.27	8.34	8.90	10.21
5	12.67	12.67	13.69	17.1

VI. ASYMPTOTIC THRESHOLD VALUES IN THE HIGH-q LIMIT

Whereas the precise values for transitions and stability regions of the 1RSB approach have to be determined by numerically solving the cavity equations, and by plugging this solution into the stability criteria, an asymptotic analysis can be carried through analytically in the limit of a large number of colors, i.e., for $q \gg 1$. As an astonishing result, Poissonian and regular random graphs have the same asymptotic behavior, at least as far as the dominant contributions are concerned. Degree fluctuations play a role only at low-order contributions which, due to the complexity of their determination, are not considered here. To lighten the presentation, we consider therefore only the case of regular graphs, i.e. of equal vertex degrees $c=k+1$ for all vertices.

As discussed above, in this case the 1RSB solution is factorized and thus completely determined by a single edge- and color-independent η. A basic numerical observation in this context is that, for $q \gg 1$, this η approaches $1/q$, whereas the probability $\eta^0=1-q\eta$ of sending a trivial message vanishes asymptotically. We can therefore write $q\eta=1-g(q,c)$, where the positive, but still unknown function $g(q,c)$ will be shown to vanish in the large-q limit.

Note that, in the case of fluctuating vertex degrees, also η will fluctuate according to some nontrivial $\rho(\eta)$. For large q, this distribution concentrates, however, more and more sharply around its average value. A careful analysis of the influence of these fluctuations shows that they contribute only to subdominant terms in the threshold values, i.e., they can be neglected to the considered orders in q.

A. The clustering transition in 1RSB approximation

The clustering transition is characterized by the onset of a nontrivial solution of the survey propagation equation (19). To determine this point, we consider a graph of constant degree $c=k+1$ with

$$k = q[\ln q + \ln\ln q + \alpha]. \tag{40}$$

There α is an arbitrary constant, i.e., in the large-q limit k is determined down to $O(q)$. Doing so, we zoom directly into the region where the dynamical transition appears: We look for an α_d at which the first nontrivial η appears as a solution of

$$\eta = \frac{\sum_{l=0}^{q-1} (-1)^l \binom{q-1}{l} [1-(l+1)\eta]^k}{\sum_{l=0}^{q-1} (-1)^l \binom{q}{l+1} [1-(l+1)\eta]^k}. \tag{41}$$

As a first step we realize that, for $\eta \simeq 1/q$ and k as given in Eq. (40), the sums in both the numerator and the denominator are dominated by values of $l \ll q$, where we can replace

$$\begin{aligned}[1-l\eta]^k &\simeq \exp\{-\eta k l\} \\ &\simeq \exp\{-[1-g(q,\alpha)][\ln q + \ln\ln q + \alpha] l\} \\ &\simeq \left[\frac{1}{q\ln q} q^{g(q,\alpha)} e^{-\alpha}\right]^l \end{aligned} \tag{42}$$

up to neglectable corrections. Note the change in notation from $g(q,c)$ to $g(q,\alpha)$. Plugging this into Eq. (41), we find

$$1-g(q,\alpha)\simeq\frac{1}{\ln q}q^{g(q,\alpha)}e^{-\alpha}\frac{\exp\left\{-\frac{1}{\ln q}q^{g(q,\alpha)}e^{-\alpha}\right\}}{1-\exp\left\{-\frac{1}{\ln q}q^{g(q,\alpha)}e^{-\alpha}\right\}}$$

$$\simeq 1-\frac{1}{2\ln q}q^{g(q,\alpha)}e^{-\alpha}. \tag{43}$$

This equation closes for $g(q,\alpha)=\gamma(\alpha)/\ln q$, with the condition

$$\gamma(\alpha)e^{-\gamma(\alpha)}=\frac{1}{2}e^{-\alpha}. \tag{44}$$

The maximum of the left-hand side is $1/e$ for $\gamma=1$, i.e., a real solution for $\gamma(\alpha)$ exists if and only if $\alpha>1-\ln 2$. We thus find the dynamical transition in the 1RSB approach at

$$c_d=q[\ln q+\ln\ln q+1-\ln 2+o(1)],$$

$$\eta_d=\frac{1}{q}\left[1-\frac{1}{\ln q}+o(\ln q^{-1})\right]. \tag{45}$$

The result is equally valid for Poissonian random graphs. This can be understood immediately: Degree fluctuations are of $O(\sqrt{c})=O(\sqrt{q\ln q})$, and they are thus neglectable compared to the contributions in Eq. (40).

B. The COL/UNCOL transition in 1RSB approximation

From the upper bound of Łuczak and the lower one of Achlioptas and Naor we know that

$$c_q\simeq 2q\ln q-\ln q+O(1). \tag{46}$$

We are going to rederive this result from the cavity equations, and we also determine the previously unknown $O(1)$ contribution. Observing that, under this scaling of the degree, the contributions in the self-consistency equation (41) behave as $[1-l\eta]^k\sim q^{-2l}$, we find

$$\eta=\frac{1}{q}\left(1-\frac{1}{2}(q-1)\left[\frac{1-2\eta}{1-\eta}\right]^k\right)+O(q^{-3})$$

$$=\frac{1}{q}\left(1-\frac{1}{2}(q-1)\exp\left\{-k\eta-\frac{3}{2}k\eta^2\right\}\right)+O(q^{-3}). \tag{47}$$

This equation is solved by

$$\eta=\frac{1}{q}-\frac{1}{2q^2}+\frac{3\ln q}{2q^3}+O(q^{-3}), \tag{48}$$

independently on the $O(1)$ term in Eq. (46). This value has to be plugged into the expression for the complexity,

$$\Sigma=\ln\left[\sum_{l=0}^{q-1}(-1)^l\binom{q}{l+1}[1-(l+1)\eta]^c\right]-\frac{c}{2}\ln(1-q\eta^2), \tag{49}$$

in order to determine the critical point c_q of the COL/UNCOL transition from the vanishing of Σ. Keeping only the three dominant terms in q, we immediately find

$$c_q\simeq 2q\ln q-\ln q-1+o(1). \tag{50}$$

The result is equally valid for Poissonian graphs, and it coincides precisely with the upper bound of Łuczak, i.e., his improved annealed approximation is asymptotically exact. It is, however, also only one larger than the conjectured lower bound by Achlioptas and Naor. In this way we see that the 1RSB approach is not only consistent with the mathematical bound, but allows for a more precise (even if not rigorous) determination of the threshold value.

C. Asymptotic stability

To check the validity of the above results, we have to certify that the 1RSB solution is locally stable. Again we discuss only the case of the regular random graph of degree $c=k+1$, but the results do not differ in the Poissonian case.

1. Instability of type I

Let us first start with the instability of type I. To do so, we should compute the eigenvalues of the stability matrix derived in Sec. IV. For average connectivities $c\gg q$, the recursion equation (15) is dominated by the first contribution in both the numerator and the denominator, leading to $\rho(\eta)=\delta(\eta-1/q)$ in leading order. Corrections are exponentially small in c/q and can thus be neglected. More precisely, taking the asymptotic $c\gg q$ results of Eq. (14) and then using the fact that all colors on all branches except the perturbed one share the same η, one obtains

$$\eta_0^\tau\simeq\frac{(1-\eta_1^\tau)(1-\eta)^{k-1}}{\sum_{\sigma=1}^q(1-\eta_1^\sigma)(1-\eta)^{k-1}}=\frac{(1-\eta_1^\tau)}{\sum_{\sigma=1}^q(1-\eta_1^\sigma)}. \tag{51}$$

We immediately compute the derivatives $(\partial\eta_0^1/\partial\eta_1^1)|_{\eta_1^\sigma\equiv\eta}$ and $(\partial\eta_0^1/\partial\eta_1^2)|_{\eta_1^\sigma\equiv\eta}$ that form the entries of the Jacobian matrix T given in Eq. (23):

$$\left.\frac{\partial\eta_0^1}{\partial\eta_1^1}\right|_{\eta_1^\sigma\equiv\eta}=-\frac{1}{q},\qquad\left.\frac{\partial\eta_0^1}{\partial\eta_1^2}\right|_{\eta_1^\sigma\equiv\eta}=\frac{1}{q(q-1)}. \tag{52}$$

Using eigenvalues (26), we finally find for $c\gg q$

$$\lambda_1=\left.\left(\frac{\partial\eta_0^1}{\partial\eta_1^1}-\frac{\partial\eta_0^1}{\partial\eta_1^2}\right)\right|_{\eta_1^\sigma\equiv\eta}\simeq-\frac{1}{q-1},$$

$$\lambda_2=\left.\left(\frac{\partial\eta_0^1}{\partial\eta_1^1}+(q-1)\frac{\partial\eta_0^1}{\partial\eta_1^2}\right)\right|_{\eta_1^\sigma\equiv\eta}\simeq 0. \tag{53}$$

Therefore, the stability criterion reads

$$\frac{k}{(q-1)^2}<1 \tag{54}$$

such that the instability appears at connectivity greater than

$$c_{\mathrm{SP}}=(1-q)^2+1\simeq q^2-2q+2+o(1). \tag{55}$$

In fact, this formula gives very good results even at small q for both Erdös-Rényi and regular random graphs. The reason

why it is working so well is that we are considering connectivities growing like q^2, so the condition $c \gg q$ is satisfied very fast.

The dominant contributions give always an integer c_{SP}. In particular in the case of regular graphs it is therefore important to know at least the sign of the next-order term. Numerically we find this to be positive for arbitrary q. Since we define c_{SP} as the first unstable connectivity, we should therefore write

$$c_{\mathrm{SP}}^{\mathrm{fixed}} = (q-1)^2 + 2. \tag{56}$$

This formula amazingly appears to be exact even for $q=3$. Note that, due to its q^2 dependence, as compared to the order $q \ln q$ of the q-COL/UNCOL transition, this instability is always located in the UNCOL phase and is thus irrelevant to the physics of the problem. It is however useful since it tells us when the SP equations at $y=\infty$ stop to converge on a single graph. The finite q result is also extremely well approximated by the $c \gg q$ limit in the case of fluctuating connectivities, giving

$$c_{\mathrm{SP}}^{\mathrm{ER}} = 1 + (q-1)^2 + o(1). \tag{57}$$

2. Instability of type II

Finally, we have also to check if a type II instability exists. To do so, we start our investigation close to the clustering transition, i.e., we go back to the scaling

$$k = q[\ln q + \ln\ln q + \alpha]. \tag{58}$$

As shown before, this results in

$$\eta = \frac{1}{q}\left[1 - \frac{\gamma}{\ln q} + o(\ln q^{-1})\right], \tag{59}$$

where γ is the smaller of the two solutions of $2\gamma e^{-\gamma} = e^{-\alpha}$. The stability criterion (38) reads

$$\lambda_{\text{type II}} = k(q-1)\frac{\sum_{l=0}^{q-2}(-1)^l\binom{q-2}{l}[1-(l+2)\eta]^{k-1}}{\sum_{l=0}^{q-1}(-1)^l\binom{q}{l+1}[1-(l+1)\eta]^{k}} < 1. \tag{60}$$

Plugging in Eqs. (58) and (59), and keeping only the leading order terms, we find

$$\lambda_{\text{type II}} = e^{\gamma-\alpha} + \mathcal{O}\left(\frac{\ln\ln q}{\ln q}\right). \tag{61}$$

For sufficiently large q, this becomes smaller than one if and only if $e^{\gamma-\alpha} < 1$ which, according to the condition for γ, holds for all $\alpha > 1/2$. We therefore conclude that 1RSB is stable for all connectivities larger than

$$c_m = q\left[\ln q + \ln\ln q + \frac{1}{2} + o(1)\right]. \tag{62}$$

This value is slightly larger than the one of c_d, i.e., there is a linearly growing gap between the onset of a nontrivial 1RSB solution and its stability. Note, however, that the relative distance of both expressions is decreasing, the two leading terms in c_d and c_m coincide.

It is very interesting to compare this behavior with the best lower bounds obtained from heuristic algorithms. As discussed in more detail in the introduction, these have the leading term $q \ln q$. This results supports the intuitive feeling that local linear-time algorithms are not able to enter the clustered phase due to the proliferation of metastable states of nonzero energy. It would be interesting to understand better the influence of the structure of the energy landscape on the behavior of local algorithms, because this interplay between static and dynamic features may be a useful tool in systematically improving algorithms.

Note in this context also that the clustered phase covers half of the COL phase for large q. This means that, compared to, e.g., $q=3$, the influence of the clustering phenomenon becomes asymptotically more and more important. In this sense, a full understanding of the clustering phenomenon beyond the 1RSB approximation is of crucial interest.

VII. THE FINITE ENERGY PHASE DIAGRAM

It is very interesting to consider also finite-energy states, both for physical and computer science motivations. Indeed, the nature of these states and their degree of RSB provide some crucial information for the physical picture of the model and for its finite-temperature phase transition. Thermodynamically, the anti-ferromagnetic Potts model on random graphs behaves, in fact, similar to a Potts glass [39,40] and it is thus interesting *per se*. For instance, one would like to know if, depending on the number of colors and on the connectivity, the system behaves as a p-spin model and has a 1RSB transition, or as the Sherrington-Kirkpatrick model which has a continuous transition. From the point of view of combinatorial optimization, it is also widely believed that the time dependence of local search algorithm, and the performance they may reach, is also related to the structure of the energy landscape [36–38]. It has been shown very recently that it is possible to predict a threshold where a slow annealing will end [14] using the statistical physics information on the nature of excited states.

The basic question we will answer in this section follows from Ref. [13], where the complexity $\Sigma(e)$ where computed using the 1RSB solution. We know now that the 1RSB solution is in fact not always correct, so we would like to know which part of the complexity curve is correct and which part is not.

A. Regular random graphs

Let us first consider regular graphs. In Fig. 7, we plot complexity versus energy, i.e., the logarithm of the number of states, divided by N, versus their energy, for 3-COL on five regular graphs, and for 4-COL on nine regular graphs. Both cases are in the COL phase which implies $\Sigma(e=0) \geqslant 0$. We already showed in this paper that the 1RSB approach is stable for these two cases at $e=0$, and therefore the computation of $\Sigma(e=0)$ is correct.

Extending our work from $e=0$ to positive energies, we indeed find that only the type-II instability is relevant in the physical part of the phase diagram (i.e., where complexity is

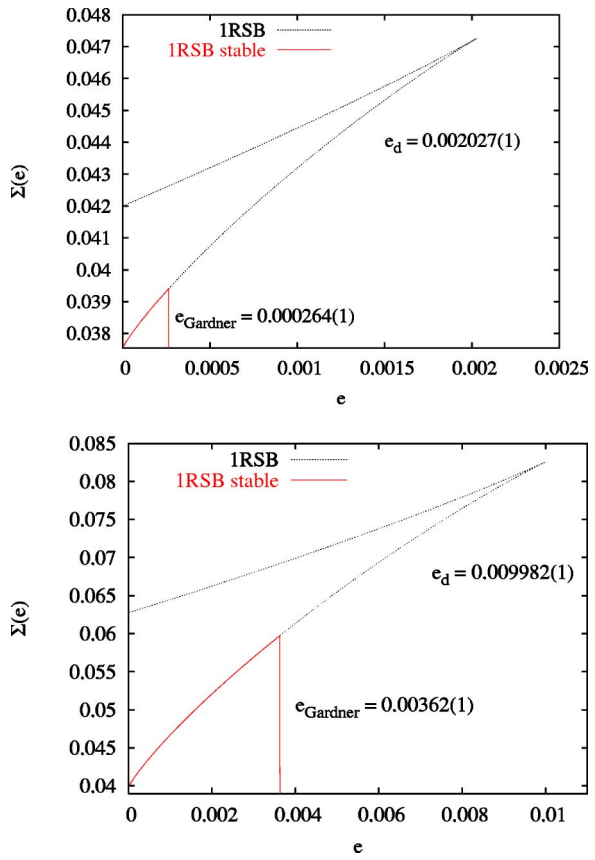

FIG. 7. (Color online) Complexity 1RSB and its 1RSB stable portion for the three-coloring problem on graph with fixed connectivity $c=5$ (left), an for the the four-coloring at $c=9$. Both system are in the COL phase, and ground state, as well as low-energy states, are described by a 1RSB ansatz. However, at high energy, when $e>e_m$, excited states should be described by a different ansatz, probably F-RSB.

non-negative). Using Eq. (34) at finite y, we observe that a large part of the positive-energy solution is 1RSB unstable, i.e., only a small fraction of the complexity curve close to the ground state is exact. Therefore, using the notation e_G (for Gardner energy [34]) for the highest energy for which 1RSB is stable, the 1RSB computation of the complexity is only valid for energies $0<e<e_G$, and should be modified for $e_G<e<e_d$.

Two questions arise. First, how to compute the correct complexity when 1RSB is unstable¿ Of course, it is in principle possible to use a 2RSB ansatz, but this is technically much more demanding, and again the stability towards 3RSB should be tested. It is still a matter of debate how to modify the complexity when 1RSB is unstable: The usual paradigm is that, if not described by 1RSB, then states should be described by a full RSB ansatz (since all known 1RSB unstable models seem to be described by full RSB). Assuming that this is indeed the case, we have to face the question of the complexity of full RSB states, which again is still very controversial. While some authors argue that full RSB states have a vanishing complexities, the question remains unsolved and has recently seen a renewed interest (see Ref. [41]).

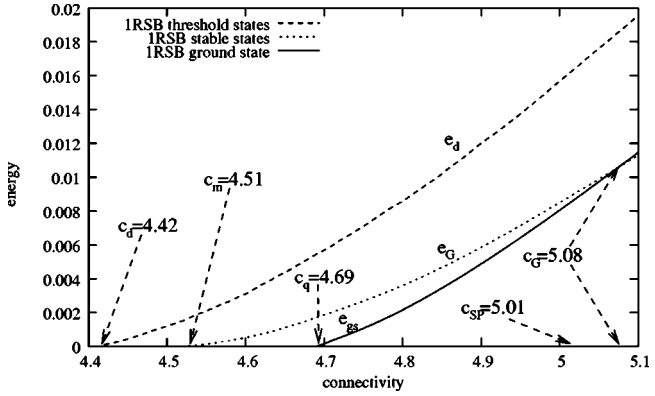

FIG. 8. Finite energy phase diagram of the three coloring. $e_{g.s.}$ gives the ground-state energy density, e_G the energy density of the 1RSB stable states of highest energy, and e_d the threshold energy in the 1RSB approximation, i.e., the energy below which a 1RSB solution exists.

Another very important question, using these complexity curves, would be to predict dynamical thresholds, as in Ref. [14]. That would be a very natural extension of this work to dynamical studies.

B. Erdös-Rényi random graphs

For Erdös-Rényi random graph, we concentrate on 3-COL. Instead of showing further complexity curves, we prefer to display, in Fig. 8, a phase diagram which we think contains a good summary of this work. The following points are to be commented on.

First, in full line, we display the ground state energy $e_{g.s.}$ versus the average connectivity c. It is zero below c_q, in the COL phase, and positive when $c>c_q\simeq 4.69$, i.e., in the UNCOL phase. This has been calculated using the energies for which the complexity is exactly zero.

The energy e_d is the threshold energy, i.e., the energy below which the clustering transition appears, and where replica symmetry is broken. In 1RSB approximation, it is nonzero for $c>c_d\simeq 4.42$.

The energy e_G is the Gardner energy, which tell us where the clustering phenomenon becomes 1RSB unstable. For $e_{g.s.}<e<e_G$, states are 1RSB stable, whereas they are unstable for $e_G<e<e_d$. This energy line starts at c_m (note that $c_d<c_m<c_q$) and allows us to determine in which zone of this phase diagram 1RSB is correct. It crosses the ground state energy line at $c_G\simeq 5.08$ (we use again the terminology of Ref. [17]; c_G stand for Gardner connectivity). Therefore, for $c>c_G$, the problem is never 1RSB (at least for physical, i.e., positive-complexity solutions).

Going back to the $e=0$ line, we have finally, in the UNCOL phase, the point where the SP equations stop to converge on a single graph. This happens for all $c\geqslant c_{SP}\simeq 5.01$.

VIII. CONCLUSION

In this paper we have studied in detail the limits of 1RSB approximation for the q-coloring problem on random graph

of both fixed and Poissonian degrees. The 1RSB approximation shows two different kind of instabilities: a type-I instability where the clusters of solutions tend to aggregate, and a type-II instability where solutions inside a cluster form further levels of clusterization. In the colorable phase, we find in particular the latter kind of instability. Luckily enough, at any $q \geqslant 3$, the COL/UNCOL transition is found in the 1RSB stable region, making it plausible that the values presented in Tables II and III are in fact the true q-COL/UNCOL thresholds.

In the limit of $q \to \infty$ many simplifications can be done in the calculation, allowing for a fully analytic treatment of the problem, and also for checking our results against the rigorous ones presented in Refs. [5,6]. We find the COL/UNCOL threshold to be asymptotically $c_q = 2q \ln q - \ln q - 1 + o(1)$ which, on the one hand, coincides precisely with the rigorous upper bound of Łuczac [5], which, on the other hand, differs only one from the lower bound of Achlioptas and Naor [6]. All these findings are good news for the 1RSB cavity approach, that not only turns out to be consistent with independently established rigorous mathematical results, but also allows for sharper, though not rigorous, determination of threshold values.

There are several lines in which the work presented here could be extended. The most straightforward direction is probably the question of how to implement a 2RSB calculation, in order to understand the phase-space structure in the 1RSB unstable region, and to see in how far the 1RSB approximations for the clustering transition, the complexity and the threshold energy have to be changed.

A second interesting direction concerns the connection between the failure of linear-time algorithms and the onset of clustering. Even if a connection between both seems pretty intuitive due to the existence of exponentially many metastable states, one should keep in mind that algorithms do not follow a physical dynamics with detailed balance, etc. The connection between the energy landscape and the configurations explored by the algorithm is therefore far from beeing obvious. Even if so far no local linear-time algorithms were found that solve q-COL inside the 1RSB stable region, their mathematical analysis has no obvious connection to the landscape properties of the model. It would therefore be extremely interesting to either establish this connection or to prove its nonexistence.

ACKNOWLEDGMENTS

We thank M. Mézard, F. Ricci-Tersenghi, O. Rivoire, and R. Zecchina for useful and cheerful discussions. We also thank the hospitality of the ICTP Trieste, and two of us (F.K. and M.W.) thank the hospitality of the ISI in Torino, where part of this work was done. We acknowledge support from the ISI Foundation, the EXYSTENCE Network, and from European Community's Human Potential program under Contract Nos. HPRN-CT-2002-00319 (STIPCO) and HPRN-CT-2002-00307 (DYGLAGEMEM).

APPENDIX A: INSTABILITY OF THE SECOND KIND

In this appendix we study the eigenvalues of the matrix V defined by Eq. (29),

$$V_{\tau\to\tilde{\tau},\sigma\to\tilde{\sigma}} = \frac{\partial \pi_0^{\tau\to\tilde{\tau}}}{\partial \pi_1^{\sigma\to\tilde{\sigma}}}. \tag{A1}$$

To compute this matrix element from Eq. (28) one needs to consider all configurations of messages $(\sigma_2, \ldots, \sigma_d)$ on the incoming links $2, 3, \ldots, d$ such that (a) if the incoming warning on link 1 is given by σ, the warning τ is induced at the output and (b) if the incoming warning on link 1 is given by $\tilde{\sigma}$, the warning $\tilde{\tau}$ is induced at the output. Since we have $q+1$ different messages labeled by $0, \ldots, q$, we have to deal with a $q(q+1) \times q(q+1)$ matrix.

A physical interpretation of recursion (8) is that, when a site is exposed to a q-component field $\vec{h} = (h^1, \ldots, h^q)$ (entries are all negative or zero, reflecting the antiferromagnetic nature of the Hamiltonian) then (i) if there is a unique maximal field component h^τ, the site will send a message $-\vec{e}_\tau$ saying "do not take color τ" via the outgoing link (in the following we call this a warning of color τ) and (ii) it will send a zero message otherwise. Let us study all elements, case by case, first when a zero message is changed to a messenger with a color, then a color is changed into another one.

1. Changing 0 to a colored message (or a color to 0)

When one changes one input message 0 to a colored one, e.g., $-\vec{e}_1$, it can be shown that most corresponding matrix elements vanish. A simple way to show it is the following: Consider link one, where we are changing the incoming message, and the other $d-1$ incoming links. In the first configuration, link one is sending a 0, so it has *no* effect. The other $d-1$ incoming messages induce a field $\vec{h}$. If we turn now the message 0 on branch one to $-\vec{e}_1$, this has the effect of decreasing field component h^1 by one. The outgoing message is nonzero only if there is a unique maximum field, this change has no effect at all if h^1 was not a maximum field component. To obtain nonzero matrix elements, we thus have to consider only situations in which this h^1 was a maximum field before changing the first message.

Two cases arise.

(1) First, if h^1 was the *only* maximum component before the change, then the output was e_1 in the first configuration. Adding a new incoming message of color one decreases h^1 by one unit. Now either h^1 is still the unique maximum, and nothing has changed, or it now equals to another field, say h^2, and the new outgoing message becomes 0. There is thus a finite probability to change the input from color 1 to 0 by changing an input 0 to color 1.

(2) Second, if h^1 was not the maximum field and if they were two such maximum fields, say h^1 and h^2, then adding an incoming message of color 1 forces h^1 to decrease, and therefore h^2 may become the only maximum and the new output is $-\vec{e}_2$.

There are thus only two nonzero terms, that we will call $\mathcal{A}$ and $\mathcal{B}$:

$$\mathcal{A} = V_{0\to 2,0\to 1},$$

$$\mathcal{B} = V_{1\to 0,0\to 1}. \tag{A2}$$

All other nonzero terms having a zero input changed to a colored one, result from simple color permutations and equal the two described ones. Note that similar equations can be written when one changes an input of color 1 to 0. In this case the only nonzero terms are given by

$$\mathcal{A}' = V_{2\to 0,1\to 0},$$

$$\mathcal{B}' = V_{0\to 1,1\to 0}. \tag{A3}$$

The values of $\mathcal{A}$, $\mathcal{A}'$, $\mathcal{B}$, and $\mathcal{B}'$ are associated to the two following situations (considering the set of fields $\vec{h}$ resulting from the other $d-1$ incoming messages): (a) $\mathcal{A}(q,\{\eta\})$ and $\mathcal{A}'(q,\{\eta\})$ are probabilities of having h^1 and h^2 as the two *only* maximum field and (b) $\mathcal{B}(q,\{\eta\})$ and $\mathcal{B}'(q,\{\eta\})$ are the probability of having h^1 as the maximum field, and that at least one other field with value $h=h^1-1$ exists. To obtain the final matrix element one has to put the reweighting factor corresponding the to second configuration, therefore we find

$$\begin{aligned}\mathcal{A}(q,\{\eta\}) &= \mathcal{A}'(q,\{\eta\}) \\ &= C_0 \sum_{(h^3,\ldots,h^q>h^1=h^2)} \tilde{P}(h^1,h^2,h^3,\ldots,h^q)e^{yh^2},\end{aligned} \tag{A4}$$

$$\mathcal{B}'(q,\{\eta\}) = C_0 \sum_{\substack{(h^2,\ldots,h^q>h^1)\\ [h^1-1=\max(h^2,h^3,\ldots,h^q)]}} \tilde{P}(h^1,h^2,h^3,\ldots,h^q)e^{yh^1},$$

$$\mathcal{B}(q,\{\eta\}) = C_0 \sum_{\substack{(h^2,\ldots,h^q>h^1)\\ [h^1-1=\max(h^2,h^3,\ldots,h^q)]}} \tilde{P}(h^1,h^2,h^3,\ldots,h^q)e^{y(h^1-1)},$$

where we have introduced, following Ref. [13], the notation $\tilde{P}(\vec{h})$ as the probability of having a configuration of messages that gives a set of fields $\vec{h}$ before any reweighting is done. Thus $\tilde{P}(\vec{h})$ would result from Eq. (17) by setting $y=0$. This notation will be of great use in the computation of Appendix A. Note that, to compute $\tilde{P}(\vec{h})$ we consider here only messages arriving from the $d-1$ unchanged links $2,3,\ldots,d$.

Finally, another very important property for the structure of the matrix is that, by changing 0 to $\tilde{\sigma}$, one cannot change a color τ to another color $\tilde{\tau}$ in the output. This will turn out to considerably simplify the problem.

2. Changing one color to another color

We now consider a change of the first incoming message from color 1 to color 2. One can show, using similar kind of reasoning, that $V_{1\to 2,1\to 2}=V_{3\to 2,1\to 2}=V_{1\to 3,1\to 2}=V_{2\to 3,1\to 2}=V_{3\to 1,1\to 2}=0$ and that $V_{2\to 1,1\to 2}=\mathcal{A}$. Having in mind these relations, we can now write the stability matrix.

3. The stability matrix *V*

We write the stability matrix V in a way that justifies why we did not care about some terms in the previous section. In the base we chose, the matrix is block triangular, so we will need only to care of diagonal block matrices to compute eigenvalues (since, in a triangular block matrix, eigenvalues are eigenvalues of the diagonal matrices). We write

$$V = \begin{bmatrix} & & (0,e)(e,0) & (e,e') \\ q\begin{cases}(0,e_1)\\(0,e_2)\\\ldots\\(0,e_q)\end{cases} & & & \\ & & M & W \\ q\begin{cases}(e_1,0)\\(e_2,0)\\\ldots\\(e_q,0)\end{cases} & & & \\ q(q-1)\begin{cases}(e_1,e_2)\\(e_2,e_3)\\\ldots\\(e_3,e_2)\\(e_2,e_1)\end{cases} & & 0 & Z \end{bmatrix}, \tag{A5}$$

where M and Z can be written

$$M = \begin{bmatrix} 0 & \mathcal{A} & \ldots & \mathcal{A} & \mathcal{B}' & 0 & \ldots & 0 \\ \mathcal{A} & 0 & \ldots & \mathcal{A} & 0 & \mathcal{B}' & \ldots & 0 \\ \ldots & \ldots & \ldots & \ldots & \ldots & \ldots & \ldots & \ldots \\ \mathcal{A} & \mathcal{A} & \ldots & 0 & 0 & 0 & \ldots & \mathcal{B}' \\ \mathcal{B} & 0 & \ldots & 0 & 0 & \mathcal{A} & \ldots & \mathcal{A} \\ 0 & \mathcal{B} & \ldots & 0 & \mathcal{A} & 0 & \ldots & \mathcal{A} \\ \ldots & \ldots & \ldots & \ldots & \ldots & \ldots & \ldots & \ldots \\ 0 & 0 & \ldots & \mathcal{B} & \mathcal{A} & \mathcal{A} & \ldots & 0 \end{bmatrix}$$

and

$$Z = \begin{bmatrix} 0 & \ldots & 0 & \mathcal{A} \\ 0 & \ldots & \mathcal{A} & 0 \\ \ldots & \ldots & \ldots & \ldots \\ \mathcal{A} & \ldots & 0 & 0 \end{bmatrix}.$$

4. Eigenvalue analysis

We are now ready to find the biggest eigenvalues of the matrix V, which will be the biggest of all eigenvalues from Z and M. The matrix Z has $(q^2-q)/2$ eigenvalues $-\mathcal{A}$, and $(q^2-q)/2$ eigenvalues $\mathcal{A}$. Eigenvalues of M can be easily studied using again its block matrix structure; the biggest one is found to be $(q-1)\mathcal{A}+\sqrt{\mathcal{B}\mathcal{B}'}$. Thus the biggest eigenvalue of the whole stability matrix is

$$\lambda = (q-1)\mathcal{A}(q,\{\eta\}) + \sqrt{\mathcal{B}(q,\{\eta\})\mathcal{B}'(q,\{\eta\})}, \tag{A6}$$

where A, B, and B' are defined by Eq. (A4). In the $y=\infty$ case, new simplification arises because $\mathcal{B}$ is associated with contradicting messages and it is annihilated by its reweighting factor. Thus

$$\lambda_{y\to\infty} = (q-1)\mathcal{A}_{y=\infty}(q,\{\eta\}), \tag{A7}$$

where $\mathcal{A}_{y=\infty}(q,\{\eta\})$ may be explicitly computed (see Appendix B) and reads

$$\mathcal{A}_{y=\infty}(q,\{\eta\}) = \frac{\sum_{l=0}^{q-2}(-1)^l\binom{q-2}{l}\prod_{i=2}^{k}[1-(l+2)\eta_i]}{\sum_{l=0}^{q-1}(-1)^l\binom{q}{l+1}\prod_{i=1}^{k}[1-(l+1)\eta_i]}. \tag{A8}$$

APPENDIX B: INSTABILITY OF THE SECOND KIND AT $y=\infty$

Let us concentrate on the *colorable phase*, where the ground states are characterized by $y=\infty$. Here we give an explicit computation of $\mathcal{A}_{y=\infty}$. Let us concentrate for the derivation for 3-COL. Following the notation of Appendix B, we denote $\tilde{P}(\vec{h})$ the probability of having a configuration of d warnings that sum up to the field $\vec{h}$ without reweighting. It has no direct physical meaning but it is of great technical help in the present computation, see Ref. [13].

We first need to calculate the value of the normalization constant C_0 in the $y\to\infty$ limit. Since reweighting is killing any term with positive energy shift, the only surviving terms in the recursion are those where all fields have at least one zero component, allowing for the selecting of at least one color without violating an edge. The normalization factor thus reads

$$\frac{1}{C_0} = \tilde{P}(0,0,0) + 3\sum_{h^1<0}\tilde{P}(h^1,0,0) + 3\sum_{h^1,h^2<0}\tilde{P}(h^1,h^2,0), \tag{B1}$$

where the combinatorial factors 3 appearing on the right-hand side are obtained by noting that $\tilde{P}(h,0,0)=\tilde{P}(0,h,0)=\tilde{P}(0,0,h)$ and that $\tilde{P}(h^1,h^2,0)=\tilde{P}(h^1,0,h^2)=\tilde{P}(0,h^1,h^2)$.

Now, we need to compute the expression for $\mathcal{A}$ from Eq. (A4), summing this time only over the $d-1$ incoming warnings $2,3,\ldots,d$2,3, in the computation of $\tilde{P}$ in the numerator

$$\mathcal{A}(q,\{\eta\}) = C_0\sum_{(h^3,\ldots,h^q<h^1=h^2=0)}\tilde{P}(h^1=0,h^2=0,h^3,\ldots,h^q). \tag{B2}$$

Therefore, $\mathcal{A}(q,\{\eta\})$ is easily computed once the expression of $\tilde{P}$ for a given number of d branches are known. Using the cavity recursion equations, one can show that, when summing over d neighbors

$$\tilde{P}(0,0,0) = \prod_{i=1}^{k}(1-3\eta_i), \tag{B3}$$

$$\sum_{h^3<0}\tilde{P}(h^3,0,0) = \prod_{i=1}^{k}(1-2\eta_i) - \tilde{P}(0,0,0) = \prod_{i=1}^{k}(1-2\eta_i) - \prod_{i=1}^{k}(1-3\eta_i), \tag{B4}$$

$$\sum_{h^1,h^2<0}\tilde{P}(h^1,h^2,0) = \prod_{i=1}^{k}(1-\eta_i) - 2\sum_{h^1<0}\tilde{P}(h^1,0,0) - \tilde{P}(0,0,0) = \prod_{i=1}^{k}(1-\eta_i) - 2\prod_{i=1}^{k}(1-2\eta_i) + \prod_{i=1}^{k}(1-3\eta_i). \tag{B5}$$

Using these relations, with the proper product over the d or $d-1$ incoming messages, we immediately get from Eq. (B2)

$$\mathcal{A}_{y=\infty}(q=3,\{\eta\}) = \frac{\prod_{i=2}^{k}(1-2\eta_i) - \prod_{i=2}^{k}(1-3\eta_i)}{3\prod_{i=1}^{k}(1-\eta_i) - 3\prod_{i=1}^{k}(1-2\eta_i) + \prod_{i=1}^{k}(1-3\eta_i)}. \tag{B6}$$

This equation can be easily generalized to an arbitrary number q of colors, and we find

$$\mathcal{A}_{y=\infty}(q,\{\eta\}) = \frac{\sum_{l=0}^{q-2}(-1)^l\binom{q-2}{l}\prod_{i=2}^{k}[1-(l+2)\eta_i]}{\sum_{l=0}^{q-1}(-1)^l\binom{q}{l+1}\prod_{i=1}^{k}[1-(l+1)\eta_i]}. \tag{B7}$$

[1] M. R. Garey and D. S. Johnson, *Computers and Intractability* (Freeman, New York, 1979).

[2] F. Y. Wu, Rev. Mod. Phys. **54**, 235 (1982).

[3] B. Bollobás, *Random Graphs* (Cambridge University Press, Cambridge, 2001).

[4] P. Erdös and A. Rényi, Publ. Math. (Debrecen) **6**, 290 (1959).

[5] T. Luczak, Combinatorica **11**, 45 (1991).

[6] D. Achlioptas and A. Naor (unpublished).

[7] Private communication with D. Achlioptas and C. Moore: Using a pretty physical symmetry assumption in the second moment method of Ref. [6], C. Moore found the conjectured lower bound. A complete proof seems, however, very hard and is still missing.

[8] E. Shamir and E. Upfahl, J. Algorithms **5**, 488 (1984).

[9] W. Fernandez de la Vega, in *Graph Theory and Combinatorics*, edited by B. Bollobás (Academic Press, New York, 1984).
[10] D. Achlioptas and M. Molloy, in *Proceedings of FOCS-97* (IEEE, New York, 1997).
[11] A. Frieze and C. J. H. McDiarmid, Random Struct. Algorithms **10**, 5 (1996).
[12] R. Mulet, A. Pagnani, M. Weigt, and R. Zecchina, Phys. Rev. Lett. **89**, 268701 (2002).
[13] A. Braunstein, R. Mulet, A. Pagnani, M. Weigt, and R. Zecchina, Phys. Rev. E **68**, 036702 (2003).
[14] A. Montanari and F. Ricci-Tersenghi, cond-mat/0401649.
[15] M. Mézard and G. Parisi, Eur. Phys. J. B **20**, 217 (2001).
[16] A. Montanari, M. Müller, and M. Mézard, Phys. Rev. Lett. **92**, 185509 (2004); M. Müller, M. Mézard, and A. Montanari, J. Chem. Phys. **120**, 11 233 (2004).
[17] A. Montanari, G. Parisi, and F. Ricci-Tersenghi, J. Phys. A **37**, 2073 (2004).
[18] A. Montanari and F. Ricci-Tersenghi, Eur. Phys. J. B **33**, 339 (2003).
[19] S. Mertens, M. Mézard, and R. Zecchina, cs.cc/0309020.
[20] O. Rivoire, G. Biroli, O. C. Martin, and M. Mézard, Eur. Phys. J. B **37**, 55 (2004).
[21] M. Molloy and B. Reed, Random Struct. Algorithms **6**, 161 (1995).
[22] M.E.J. Newman, S.H. Strogatz, and D.J. Watts, Phys. Rev. E **64**, 026118 (2001).
[23] M. Mézard and G. Parisi, J. Stat. Phys. **111**, 1 (2003).
[24] M. Mézard, G. Parisi, and R. Zecchina, Science **297**, 812 (2002).
[25] M. Mézard and R. Zecchina, Phys. Rev. E **66**, 056126 (2002).
[26] F. Guerra and F.L. Toninelli, Markov Processes Relat. Fields **9**, 195 (2003).
[27] S. Franz and M. Leone, J. Stat. Phys. **111**, 535 (2003); cond-mat/0208280.
[28] D. Sherrington and S. Kirkpatrick, Phys. Rev. Lett. **35**, 1792 (1975).
[29] M. Talagrand, C. R. Acad. Sci. **337**, 111 (2003).
[30] B. Derrida, Phys. Rev. Lett. **45**, 79 (1980).
[31] M. Mezard, F. Ricci-Tersenghi, and R. Zecchina, J. Stat. Phys. **111**, 505 (2003).
[32] S. Cocco, O.Dubois, J. Mandler, and R. Monasson, Phys. Rev. Lett. **90**, 047205 (2003).
[33] Note that the local stability of the 1RSB solution is necessary, but not sufficient for demonstrating its correctness. Up to now, however, no model was found which shows a discontinuous transition from 1RSB to a more-step solution. Based on this experience we conjecture a locally stable 1RSB solution to be in fact the exact solution.
[34] E. Gardner, Nucl. Phys. B **257**, 747 (1985).
[35] C. De Dominicis, T. Temesvari, and I. Kondor, J. Phys. IV (France) **8**, 13 (1998); Eur. Phys. J. B **11**, 629 (1999).
[36] O. Dubois, R. Monasson, B. Selman, and R. Zecchina, Theor. Comput. Sci. **265**, special issue (2001).
[37] R. Monasson, Phys. Rev. Lett. **75**, 2847 (1995).
[38] D. Thirumalai and T. R. Kirkpatrick, Phys. Rev. B **38**, 4881 (1988).
[39] D. J. Gross, I. Kanter, and H. Sompolinsky, Phys. Rev. Lett. **55**, 304 (1985).
[40] K. Binder and A. P. Young, Rev. Mod. Phys. **58**, 801 (1986); M. Mézard, G. Parisi, and M. A. Virasoro, *Spin Glass Theory and Beyond* (World Scientific, Singapore 1987); K. H. Fisher and J. A. Hertz, *Spin Glasses* (Cambridge University Press, Cambridge, 1991); *Spin Glasses and Random Fields*, edited by A. P. Young (World Scientific, Singapore, 1998).
[41] A. Annibale, A. Cavagna, I. Giardina, G. Parisi, and E. Trevigne, cond-mat/0307465; T. Aspelmeier, A. J. Bray, and M. A. Moore, cond-mat/0309113; A. Crisanti, L. Leuzzi, G. Parisi, and T. Rizzo, cond-mat/0309256; A. Cavagna, I. Giardina, and G. Parisi, cond-mat/0312534; G. Parisi and T. Rizzo, cond-mat/0401509.